M&C 2017 - International Conference on Mathematics & Computational Methods Applied to Nuclear Science & Engineering, Jeju, Korea, April 16-20, 2017, on USB (2017)

Developments of the sodium fast reactor analysis code SARAX: methods and verification

Xianan Du, Liangzhi Cao, Youqi Zheng*, Hongchun Wu

School of Nuclear Science and Technology, Xi'an Jiaotong University, Xi'an 710049, China
dxndxnwww@stu.xjtu.edu.cn
caolz@mail.xjtu.edu.cn
yqzheng@mail.xjtu.edu.cn
hongchun@mail.xjtu.edu.cn

Abstract - *A new code system named SARAX for the fast reactor design and fuel cycle analysis was recently developed. The SARAX system mainly consists of two parts. The few group constants were generated by the SARAX-FXS code and the steady-state, fuel cycle and transient calculations were done by the SARAX-FR code. This paper presents the models adopted in the new codes and the verification test problem results are given to show the current capability and accuracy. The verifications are based on the OECD fast reactor benchmarks, which consist of four difference fast reactor designs. The few group cross sections, keff and power distribution were calculated with different models of generating few group constants. The results were compared with a continuous energy Monte-Carlo calculation. The relative differences of keff between SARAX and the reference code were less than 100pcm for the large size cores and 300pcm for the medium size cores. The RMS value of power distribution was less than 3%. Besides, the Doppler constants, void worth, control rod worth and reactivity swing were also calculated and compared.*

I. INTRODUCTION

The numerical method for fast reactor core analysis is continuously developed in the past decades. Compared with thermal reactor, the fast reactor has very different neutronic behaviors. In the fast reactor, the averaged neutron energy of fast reactors is much higher than that of thermal reactors, which makes the anisotropic angular distribution of elastic scattering more important. Meanwhile, the scattering resonances of medium mass nuclides makes the neutron spectrum more jugged and complex in the high energy range [1]. These features encourage the new development of a dedicated code for fast reactor analysis.

According to the different methods used in the few-group constants' generation, the numerical methods for fast reactor analysis could be divided into two ways: the hybrid way and the deterministic way. In hybrid way, a lot of efforts have been made to introduce the Monte Carlo method into the fast reactor cross section generation. From 2013, the Serpent code was combined with the DYN3D/PARCS codes to analyze the Sodium cooled Fast Reactor (SFR) and the results were in good agreement with the reference results [2-4]. In their studies, the 3D sub-assembly and super cell sub-assembly models were built to generate the few group cross sections for different assembly. Besides, Heo et al. did similar works and obtained promising results by using the MCNP5 and DIF3D codes [5]. To consider the global coupling effect, a special equivalent homogeneous RZ core model was built to calculate the homogenized cross sections in the study. In the deterministic way, the Bondarenko self-shielding factor method [6] was widely used in generation the self-shielding cross sections in last century. In recent years, the following development of cross section generation focused on the rigorous treatment of energy variable and the finer neutron spectrum expression was applied. The ECCO [7] code improved the self-shielding factor method by utilizing more energy groups (1968-group) and combined the sub-group method in the lattice analysis. The EXUS-f [8] code used point-wise ENDF (PENDF) library directly for the important nuclides to consider the resonance effect, such as ^{23}Na, ^{56}Fe, ^{238}U and ^{239}Pu. In MC^2-3 [1,9] code that was developed at Argonne National Laboratory (ANL), the ultrafine group (~2000) or the hyperfine group (~400,000) calculation was done optionally to obtain the detailed neutron spectrum.

In China, a new code system called SARAX (System for fAst Reactor Analysis at Xi'an Jiaotong University) was designed for the fast reactor steady-state, fuel cycle and transient calculations [10]. In the previous version, SARAX invoked the OpenMC [11] Monte Carlo code to generate assembly few-group cross sections. Then, the 3D whole core calculation would be done by the DNTR [12] code, which was based on the 3D S_N nodal transport method. However, some weaknesses were encountered during the application. Because of using the Monte Carlo method for cross section generation, it is very inefficient. Moreover, the generation of higher order scattering matrices is very difficult in using the Monte Carlo method. Additionally, the DNTR code could only run with one calculation core.

Therefore, some improvements were introduced in the current version of SARAX [13,14]. Firstly, the more efficient and flexible deterministic method was used in the few group constants generation. Then, the core calculation was extended to have parallel capability for the angular sweeping.

In this paper, we briefly introduce the new features of current SARAX and show the results of 4 OECD fast reactor benchmarks to verify the accuracy. The k_{eff}, power distribution and reactivity coefficient parameters were compared with the reference Monte-Carlo calculations. The results show good agreements with references.

II. SARAX CODE SYSTEM

The SARAX code system is mainly consists of two parts: SARAX-FXS and SARAX-FR. The SARAX-FXS code can generate the assembly few-group cross sections with homogeneous model and 1D slab/ cylinder heterogeneous models. Optionally, the 2D RZ calculation using the S_N method will be performed model the interference of different material zone and leakage. The SARAX-FR code will perform the steady-state core calculation, depletion calculation, reactivity coefficient calculation and transient calculation with different input option. The transport solver is based on DNTR code. The output files are in the VTK or HDF5 format.

1. SARAX-FXS

In the current SARAX-FXS code, the neutron spectrum within a group is used to consider the elastic scattering resonance effect and interference effect accurately. The point-wise data from PENDF is used in the calculation here. Based on this idea, the traditional equivalence theory is applied and improved. Fig. 1 shows the flow chart in SARAX-FXS.

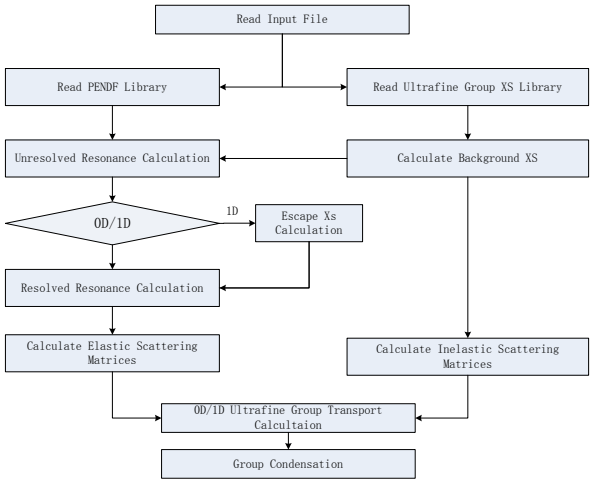

Fig. 1. Computational Flow of SARAX-FXS code

1.1. Preparation of ultrafine group cross sections

The NJOY [15] code is used to produce the PENDF and ultrafine group library for each nuclide based on the ENDF/B-VII.0 library. In the PENDF library, the total, elastic scattering, fission, capture cross sections as functions of energy point and temperature are generated. In the unresolved resonance region, the cross sections are defined as a function of background cross section and energy at each temperature. In the ultrafine group library, the ultrafine-group cross sections as functions of background cross section and temperature are generated in the MATXS format. In this paper, we apply the 1968-group structure for the ultra-fine group library. The upper and lower energy bounds of energy are 19.6MeV and 0.0001eV, respectively.

The SARAX-FXS code reads cross sections from the pre-generated ultrafine group library for specified compositions. Since the inelastic scattering cross sections don't have significant resonance effect, the macroscopic inelastic scattering matrices are calculated using the production of number density and microscopic cross section of each nuclide. The background cross section σ_0^i for isotope i is calculated as follows:

$$\sigma_0^i = \sum_{j \neq i} N_j \sigma_t^j / N_i \tag{1}$$

where N_i and N_j are the nuclide density of isotope i and j, and σ_t^j is the microscopic total cross section of isotope j.

Then, SARAX-FXS reads the total, elastic scattering, fission, capture cross sections from the PENDF library. In the unresolved resonance region, the calculated background cross sections are applied to interpolate the total, elastic scattering, fission, capture cross sections. For the resolved resonance self-shielding cross sections, following definition is used:

$$\bar{\sigma}_{x,g}^i = \int_{\Delta E_g} \sigma_x^i(E) f(E)\, dE \Big/ \int_{\Delta E_g} f(E)\, dE \tag{2}$$

where $\bar{\sigma}$ is the homogeneous cross section and the subscript x and g are the indices for reaction type and energy group, respectively.

Based on the narrow resonance (NR) approximation, the self-shielded cross section in the homogeneous mixture is obtained as:

$$\bar{\sigma}_{x,g}^i = \int_{\Delta E_g} \frac{\sigma_x^i(E)}{\sigma_t(E)} dE \Big/ \int_{\Delta E_g} \frac{1}{\sigma_t(E)} dE \tag{3}$$

To consider the heterogeneous effect, the escape cross section will be calculated by using the CPM method [16], then the self-shielded cross section in the heterogeneous model will be obtained as:

$$\bar{\sigma}_{x,g} = \frac{\int_{\Delta E_g} \frac{\sigma_x(E)}{\Sigma_t(E) + \Sigma_e(E)} dE}{\int_{\Delta E_g} \frac{1}{\Sigma_t(E) + \Sigma_e(E)} dE} \tag{4}$$

The elastic scattering transfer cross section will be calculated on the fly by using the elastic scattering cross section in group g and a pre-calculated function $F(l, \alpha, g \to g')$, which depends on nuclide and energy structure:

$$\sigma_s^l(g \to g') = \sigma_{s,g} F(l, \alpha, g \to g') \tag{5}$$

where

$$F(l,\alpha,g\to g')=\frac{1}{\Delta E_g(1-\alpha)}\int_{\Delta E_g}dE\int_{\Delta E_{g'}}dE'\frac{P_l(\mu_s)}{E}\sum_{n=0}^{N}\frac{2n+1}{2}a_n(E)P_n(\mu_c)$$

1.2. Ultrafine-group spectrum calculation

For a homogeneous mixture, by using the P_N approximation and extended transport approximation, the neutron spectrum can be obtained as follows:

$$iB\phi_1^g+\Sigma_t^g\phi_0^g=\sum_{g'}\Sigma_{s,0}^{g'-g}\phi_0^{g'}+S_f^g+S_{ex}^g \tag{6}$$

$$\frac{iB}{3}\phi_0^g+A_1^g\phi_1^g=\sum_{g'}\Sigma_{s,1}^{g'-g}\phi_1^{g'} \tag{7}$$

$$\phi_n^g=-\frac{n}{(2n+1)A_n^g}iB\phi_{n-1}^g,n=2,...,N \tag{8}$$

$$A_n^g=b_{n-1}^g+\frac{a_n}{A_{n+1}^g}=b_{n-1}^g+\cfrac{a_n}{b_n^g+\cfrac{a_{n+1}}{\cdots+\cfrac{a_{N-1}}{b_{N-1}^g}}} \tag{9}$$

$$a_n=\frac{n+1}{2n+1}\frac{n+1}{2(n+1)+1}B^2 \tag{10}$$

$$b_n^g=\Sigma_t^g-\Sigma_{s,n+1}^g \tag{11}$$

where $\Sigma_{s,l}^{g'-g}$ is the scattering transfer cross section of order l from a source group g' to a sink group g, Σ_t^g is the total cross section, ϕ_l^g is the neutron flux of order l, S_f^g and S_{ex}^g are respectively the fission source and external source. B^2 is the buckling.

In the 1D slab or cylinder model, the ultrafine neutron spectrum can be calculated by using the CPM method:

$$\phi_{g,i}=\sum_{j=1}^{I}[\sum_{g'=1}(\Sigma_s^{j,g'-g}+\frac{\chi_g}{k}\upsilon\Sigma_{f,j,g'})\phi_{g',j}]\frac{P_{ij,g}V_j}{\Sigma_{t,i,g}V_i} \tag{12}$$

where the subscript i and j denote the region number, P_{ij} is the collision probability, V_i is the volume of region i.

2. SARAX-FR

The SARAX-FR code applies the S_N nodal transport method in triangular-z geometry. The neutron transport equation is written in standard notation as:

$$\mu^m\frac{\partial\psi^m(x,y,z)}{\partial x}+\eta^m\frac{\partial\psi^m(x,y,z)}{\partial y}+\frac{\xi^m}{h_z}\frac{\partial\psi^m(x,y,z)}{\partial z}+\Sigma_t\psi^m(x,y,z)=Q(x,y,z) \tag{13}$$

Where, $\psi^m(x,y,z)$ is the neutron flux at location(x,y,z),$h_z$is the nodal height, $\mu^m,\eta^m,\xi^m$are the direction cosine relative to the x,y and z directions.

The coordinate transformation is used to transform an arbitrary triangle into a regular triangle in the computational coordinate(x',y',z) (see in Fig.. 2). The expression can be written as:

$$x=\frac{x_1+x_2+x_3}{3}+(-x_1+\frac{x_2+x_3}{2})x'+\frac{\sqrt{3}(-x_2+x_3)}{2}y'$$
$$y=\frac{y_1+y_2+y_3}{3}+(-y_1+\frac{y_2+y_3}{2})x'+\frac{\sqrt{3}(-y_2+y_3)}{2}y' \tag{14}$$

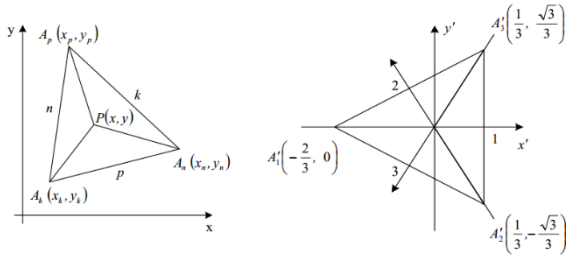

Fig. 2.Initialize Arbitrary Triangle (left) and Regular Triangle in the New Coordinate (right)

Using Eq. (14), Eq. (13) becomes as:

$$\mu_x^m\frac{\partial\psi^m(x',y',z)}{\partial x}+\eta_x^m\frac{\partial\psi^m(x',y',z)}{\partial y}+\frac{\xi^m}{h_z}\frac{\partial\psi^m(x',y',z)}{\partial z}+\Sigma_t\psi^m(x',y',z)=Q(x',y',z) \tag{15}$$

Where:

$$\mu_x^m=\frac{(-y_2+y_3)\mu^m+(x_2-x_3)\eta^m}{2\Delta}$$
$$\eta_x^m=\frac{(-x_1+1/2x_2+1/2x_3)\eta^m+(y_1-1/2y_2-1/2y_3)\mu^m}{\sqrt{3}\Delta}$$

For the transient calculation, three different kinetics methods are implemented in the SARAX-FR code, including the backward finite difference method [17], predictor-corrector quasi-static method [18] and point kinetics approximation [19]. Additionally, the parallel channel thermal hydraulic model is coupled to the neutronic calculations to consider the effect of feedback in some cases.

In SARAX-FR code, the solution method consists of the five layers of iteration:

--- Fission source iteration
  --- Iteration over energy groups
    --- Scattering iteration
      --- Angular sweeping
        --- Mesh sweeping

Since the coupling between the angles is rather weak in S_N method, it is convenient to achieve the parallel calculation in angular sweeping. Therefore, in SARAX-FR, the parallel calculation is performed in the angular sweeping by using OpenMP shared-memory parallelism. When no reflected boundary condition is present, the sweeping for each angle could start at the same time. When reflected boundary conditions are present, the number of the angular

sweeping that start at the same time should be decreased to half. It should be noticed that the numbers of computational processors used in parallel calculation were limited.

III. NUMERICAL RESULTS

1. Description of the benchmarks and SARAX calculation model

According to the Sodium-cooled Fast Reactor (SFR) Benchmarks of OECD/NEA [20], four SFR benchmarks were selected in the verification of SARAX code system. Among them, two large size core designs were proposed by CEA, which generate 3600 MW(th) and adopted the oxide and carbide fuels (MOX-3600 and CAR-3600). Two medium size core designs were proposed by ANL, which generate 1 000 MW(th) and adopted the oxide and metallic fuels.

The continuous energy OpenMC Monte Carlo calculation was performed to generate the reference results. For the reference calculations, the homogeneous core was modeled in current tests. For each case, 400 million active neutron histories were used in the Monte-Carlo calculations.

In the SARAX calculations, two models were used in generating the few group cross sections: 1) the buckling model, 2) the RZ equivalent core model.

In the buckling model, the fuel assemblies were calculated with homogeneous model and the 26-group cross sections were condensed by the homogeneous neutron spectrum. For the control rod assembly and reflector assembly, the critical buckling search calculation for fuel assembly was done firstly and the leakage spectrum was obtained. Then the leakage spectrum was applied in the homogeneous fixed source calculation and the neutron spectrum for structural material zone could be calculated.

In the RZ equivalent core model, the SARAX-FXS code only generated the 1968-group cross sections for each assembly. For precise consideration of neutron leakage, after preparing the ultrafine group cross sections, a 2D RZ equivalent core model would be built and the 1968-group S_N transport calculation would be done. By using the space-dependent neutron spectrum as the weight function, the cross sections were condensed into 26 groups. The group structure is shown in table 1.

Table 1. 26-Group Structure

Group number	Upper energy limit, MeV	Group number	Upper energy limit, MeV
1	1.9600e+01	14	2.4788e-02
2	1.0000e+01	15	1.5034e-02
3	6.0653e+00	16	9.1188e-03
4	3.6788e+00	17	5.5309e-03
5	2.2313e+00	18	3.3546e-03
6	1.3534e+00	19	2.0347e-03
7	8.2085e-01	20	1.2341e-03
8	4.9787e-01	21	7.4852e-04
9	3.0197e-01	22	4.5400e-04
10	1.8316e-01	23	3.1203e-04
11	1.1109e-01	24	1.4894e-04
12	6.7379e-02	25	9.1661e-05
13	4.0868e-02	26	6.7904e-05

As the trade-off of accuracy and efficiency, the SARAX-FR calculations were performed using the S_4 approximation. Each assembly was divided into 6 triangular meshes and the height of each nodal was ~15cm.

2. Results and discussion

Table 2 summarizes the comparison of k_{eff} value for different problems. For the two large size cores, the relative differences of k_{eff} based on the buckling model are less than 300pcm. When using the RZ model, the results get better and the relative differences are less than 100pcm. For the two medium size cores, because of stronger leakage, the buckling model could not give the accurate results. The relative differences are more than 600pcm. When using the RZ model, the relative differences decrease to 300pcm.

Table 2. Summary of k_{eff} value

		OpenMC	buckling	RZ
MOX-3600	k_{eff}	1.00629	1.00372	1.00581
	Rel.diff / pcm		-255	-47
CAR-3600	k_{eff}	0.99805	0.99537	0.99729
	Rel.diff / pcm		-270	-76
MET-1000	k_{eff}	1.02442	1.01509	1.02128
	Rel.diff / pcm		-898	-300
MOX-1000	k_{eff}	1.02246	1.01620	1.01919
	Rel.diff / pcm		-602	-314

To further analyze the differences between these two models, the 26 group macroscopic total cross sections and power distribution of MET-1000 core are compared. The distribution of materials loaded in active core is shown in Fig. 3. Fig. 4 to Fig. 7 shows the relative differences of 26 group macroscopic total cross sections between references and SARAX calculations with different model. The reference results were calculated by OpenMC code with homogeneous core model. For the fuel zones, the relative differences of few-group total cross sections calculated by the buckling model are about 1%, and in the last 4 groups, the differences are more than 2% for some zones. Obviously in Fig. 4, the situation gets worse in the structural material zones, the maximum value is almost 8%. By using the RZ model, the relative differences decrease remarkably. Less than 1% relative difference is obtained mostly. Since the RZ model is an equivalent model compared with the real core model, the leakage obtained from this model is closer to the actual situation. Therefore, the RZ model gives more accurate results than the buckling model does.

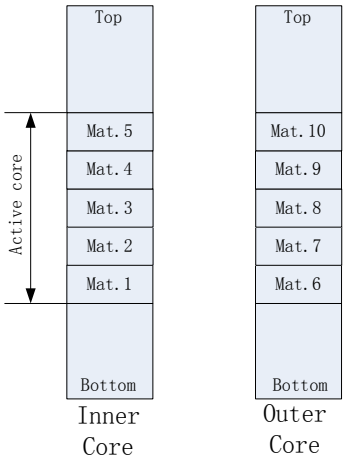

Fig. 3. The relative difference of macroscopic total cross section in fuel zones with buckling model

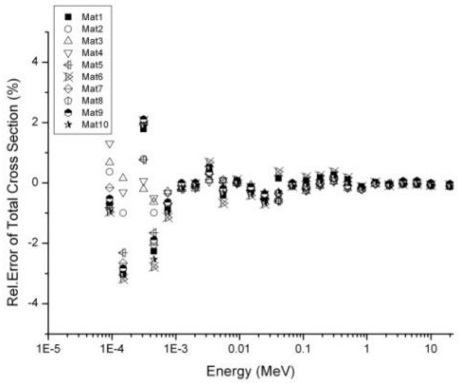

Fig. 4. The relative difference of macroscopic total cross section in fuel zones with buckling model

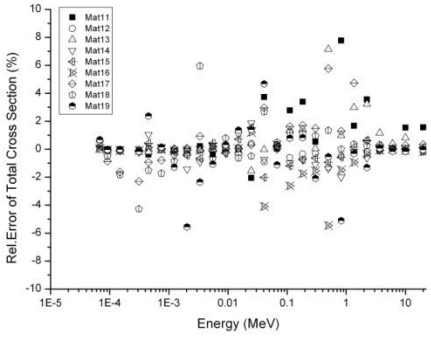

Fig. 5. The relative difference of macroscopic total cross section in structural material zones with buckling model

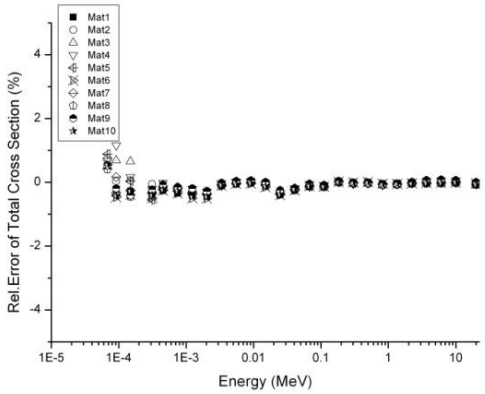

Fig. 6. The relative difference of macroscopic total cross section in fuel zones with RZ model

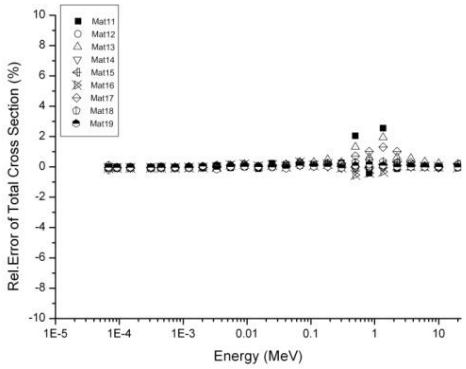

Fig. 7. The relative difference of macroscopic total cross section in structural material zones with RZ model

For the power distribution comparisons, the RZ model (as in Fig. 9) also shows better accuracy than the buckling model (as in Fig. 8). The RMS value of assembly power by using the RZ model is 1.75% while that of buckling model is 2.38%.

The void worth, Doppler constant, control rod worth and reactivity swing of MOX-3600 and CAR-3600 core were calculated and compared as in Figs. 10-17. All the calculations were done with RZ model. The results calculated by OpenMC and SARAX are marked in red, and the results from the other participants are shown in blue. The participants are divided into two kinds, the one is based on the Monte Carlo method and the other is based on deterministic method. Table 3 shows the calculation method employed by the other participants.

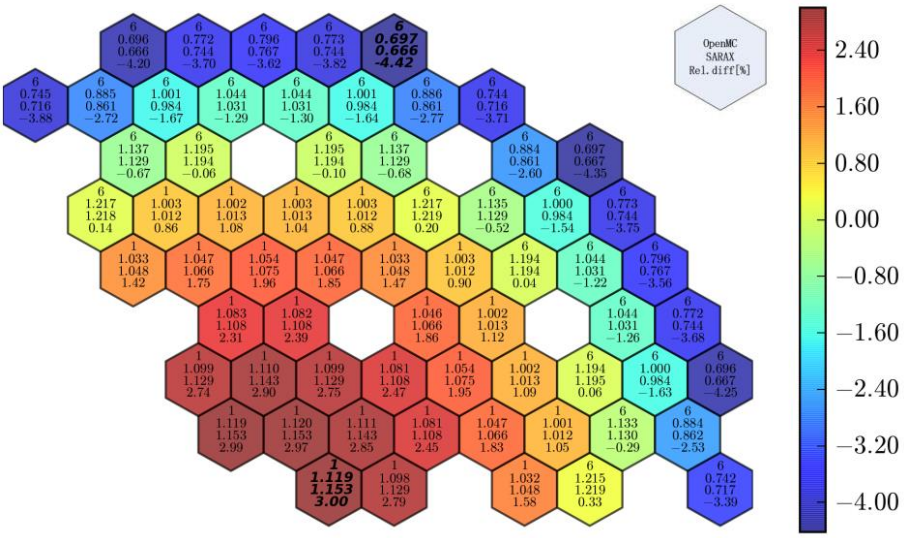

Fig. 8. The power distribution of buckling model and its relative differences

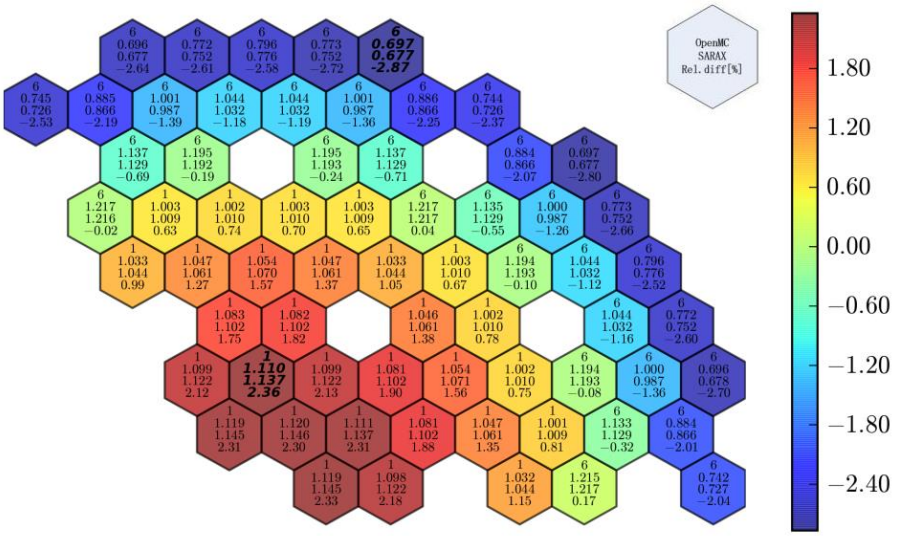

Fig. 9. The power distribution of RZ model and its relative differences

Table 3. Summary of the calculation method employed by the participants

	Participant	Library	Code
Monte Carlo method	ENEA	ENDF/B-VII.0	MCNPX
	HZDR	ENDF/B-VII.0	SERPENT
	CEA-10	JEFF-3.1.1	TRIPOLI-4
	JAEA-3	JENDL-4.0	MVP
	ANL-2	ENDF/B-VII.0	MCNP5
	ANL-3	JEFF-3.1	MCNP5
Deterministic method	ANL-1	ENDF/B-VII.0	MC^2-3/ REBUS-3
	ANL-4		ECCO/ ERANOS
	CEA-7		ECCO/ ERANOS

Compared with the OpenMC reference calculation, the void worth calculated by SARAX has discrepancy less than 100pcm. However, the value is higher than all other participants' results.

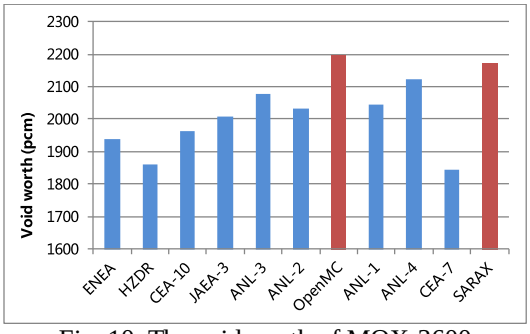

Fig. 10. The void worth of MOX-3600

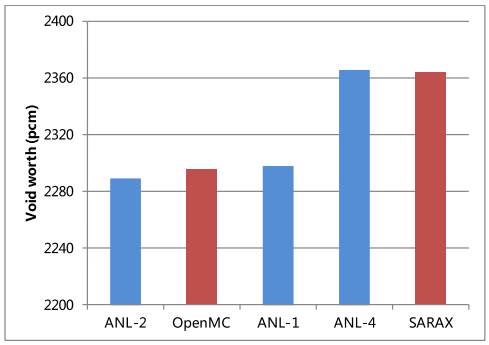

Fig. 11. The void worth of CAR-3600

The Doppler constant calculated by SARAX is -915 for the MOX-3600 core, and that is -914 for the CAR-3600 core. These values are little smaller than the average value. The control rod worth calculations are almost the same between the SARAX calculation and the OpenMC calculation, but they are both less than the ANL's results. Similar results can also been observed in the reactivity swing calculations. In summary, compared with the OpenMC reference calculations, the SARAX calculations obtain the results with high accuracy.

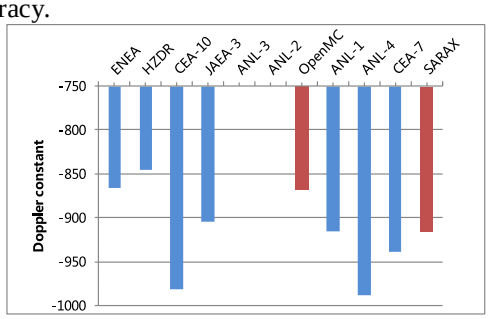

Fig. 12. The Doppler constant of MOX-3600

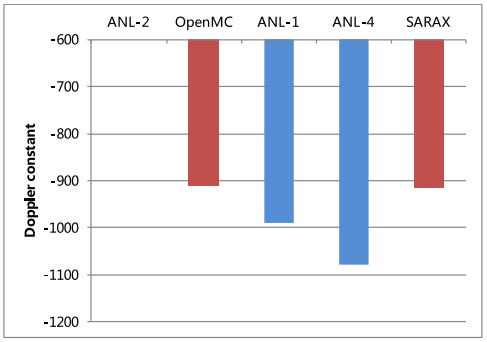

Fig. 13. The Doppler constant of CAR-3600

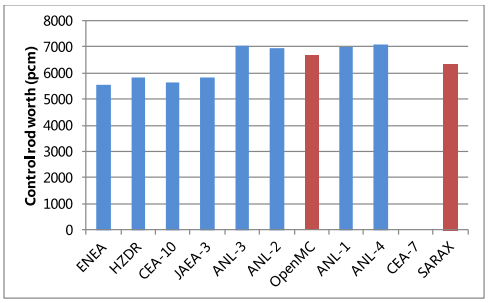

Fig. 14. The control rod worth of MOX-3600

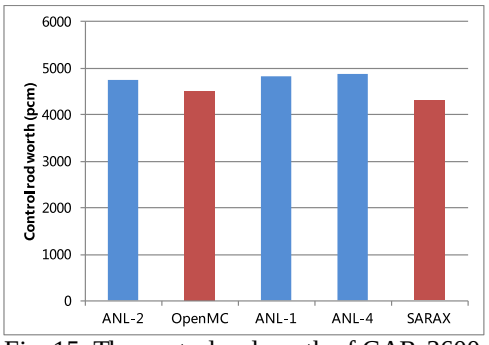

Fig. 15. The control rod worth of CAR-3600

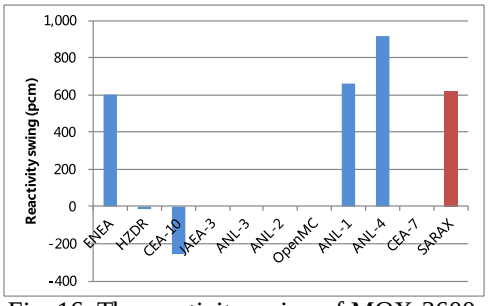

Fig. 16. The reactivity swing of MOX-3600

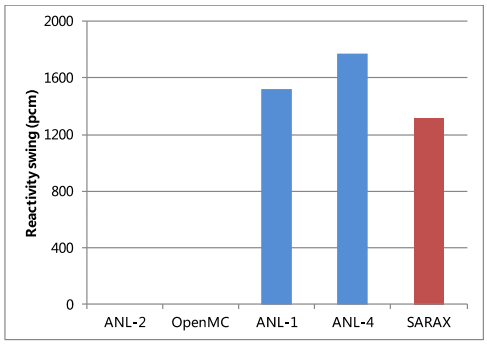

Fig. 17. The reactivity swing of MOX-3600

Fig. 18 shows the time consumption of MOX-3600 case is calculated with different numbers of computational processors. In each calculation, 41838 meshes were calculated with S_8 approximation. The system used in calculations is the personal computer consisting of Intel Core i7-2600 3.40 GHz and 8 GB memory. Obviously, the SARAX-FR calculation saves a lot of time by using multi-processors. When two processors are applied, 46.5% of

calculation time is saved. Even the number of processor reaches the maximum, the parallel efficiency is still about 90.5%.

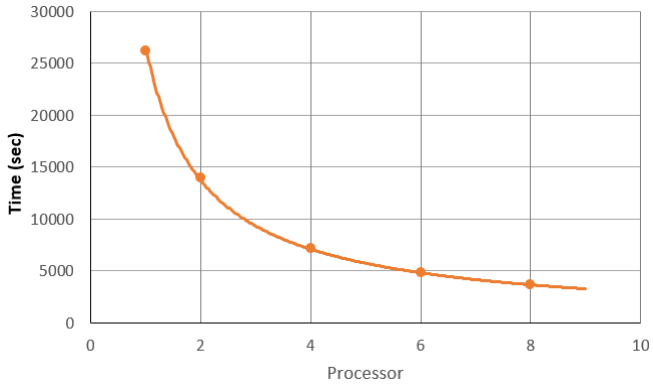

Fig. 18. Time consumption of MOX-3600 case

IV. CONCLUSION

A new dedicated code system, SARAX, was recently developed for the fast reactor analysis. In this paper, the methods used in the SARAX code system are described. In the verification, four SFR benchmarks designed by CEA and ANL were calculated and compared with reference calculations.

The results obtained by using different leakage models are analyzed. For large size cores, the leakage is not so strong that the buckling model can give acceptable results. However, for the medium size cores, the leakage of neutron is much stronger. The RZ equivalent core model is necessary, which brings much better accuracy. The k_{eff} values, the few-group cross sections and the power distributions are both in good agreement with the reference results.

For the comparisons of other neutronic results, like the Doppler constants, void worth, control rod worth and reactivity swing during the core life, the SARAX code system can also give good results compared with the references. It proves that the SARAX code system has been capable of handling preliminary fast reactor design works. Furthermore, the parallel capability in the angular sweeping makes fast reactor design works more efficient.

ACKNOWLEDGMENTS

This work is supported by the National Natural Science Foundation of China (grant number 11475134, 11522544).

REFERENCES

1. W.S. Yang. Fast Reactor Physics and Computational Method[J]. Nuclear Engineering and Technology, 2012, **44**(2):177-198.
2. R. Rachmin, C. Wemple, E. Fridman. Neutronic analysis of SFR core with HELIOS-2, Serpent, and DYN3D codes[J]. Annals of Nuclear Energy, 2013, 55:194-204.
3. E. Nikitin, E. Fridman, K. Mikityuk. Solution of the OECD/NEA neutronic SFR benchmark with Serpent-DYN3D and Serpent-PARCS code systems[J]. Annals of Nuclear Energy, 2015, 75:492-497.
4. E. Fridman, E. Shwageraus. Modeling of SFR cores with Serpent – DYN3D codes sequence [J]. Annals of Nuclear Energy, 2013, 53:354-363.
5. W. Heo, W. Kim, Y. Kim. Feasibility of a Monte Carlo-Deterministic Hybrid Method for Fast Reactor Analysis[C]. M&C2013, May 5-9, 2013, Sun Valley, Idaho, USA.
6. I.I. Bondarenko. Group Constants for Nuclear Reactor Calculations. Consultans Bureau Enterprises, Inc., New York, 1964.
7. J.M. Ruggeri, J. Tommasi, J.F. Lebrat, et al., ERANOS 2.1: The International Code System for GEN-IV Fast Reactor Analysis [C], ICAPP 2006, Reno, Nevada, USA.
8. C.H. Lim, H.G. Joo, W.S. Yang. NJOY Based Multigroup Cross Section Generation for Fast Reactor Analysis[C]. M&C2015, April 19-23, Nashville, TN, USA.
9. W.S. Yang, M.A. Smith, C.H. Lee, et al., Neutronics Modeling and Simulation of SHARP for Fast Reactor Analysis[J]. Nuclear Engineering and Technology, 2010, 42(5):520-545.
10. Zheng Youqi, Wu Hongchun, NECP team. Development of NECP-SARAX1.0 Code for Fast Reactor Physics Calculation [J]. Nuclear Power Engineering, 2014,**35**(S2):116-118. (In Chinese)
11. MIT Computational Reactor Physics Group. OpenMC Monte Carlo Particle Transport Code, https://github.com/mig-crpg/openmc, 2012.
12. Haoliang Lu, Hongchun Wu. A Nodal SN Transport Method for the Three-Dimensional Triangular-z Geometry[J]. Nuclear Engineering and Design, 2007, **237**(8): 830-830.
13. Xianan Du, Liangzhi Cao, Youqi Zheng. The Generation of Few-group Constants for Fast Reactor[C]. ICONE24, Charlotte, North Carolina, USA, 2016.
14. Xianan Du, Liangzhi Cao, Youqi Zheng. The study on the method of generating the homogenized fast reactor assembly constants based on point-wise cross section[C]. Corphy2016, Beijing, China, 2016. (In Chinese)
15. R.E. MafFarlane, D.W. Muir, A.C. Kahler. The NJOY Nuclear Data Processing System, Version 2012[R]. LA-UR-12-27079, Los Alamos National Laboratory, 2012.
16. Dan Gabriel Cacuci. Handbook of Nuclear Engineering [M]. ISBN: 978-0-387-98137-7, 2010.
17. B. Tyobeka, A. Pautz, K. Ivanov. Application of time-dependent neutron transport theory to high-temperature reactors of pebble bed type. Nucl. Sci. Eng, 168(2):93-114, 2011.

18. S. Dulla, E.H. Mund, P. Ravetto. The quasi-static method revisited. Prog. Nucl. Energy, 50, 908-920, 2008.
19. B. Ganapol, P. Picca, A. Previti, et al., Benchmarks for the Point Kinetics Equation, M&C2013, Sun Vally, 2013.
20. OECD/NEA. Benchmark for Neutronic Analysis of Sodium-cooled Fast Reactor Cores with Various Fuel Types and Core Sizes[R]. 2016.